Investigating the pathogenicity of the recessive *HNF1A* p.A251T variant in monogenic diabetes using iPSC-derived beta-like cells

Ines Cherkaoui[1,2], Qian Du[3], Dieter M. Egli[3], Camille Dion[4], Harry G. Leitch[4,5], Dilshad Sachedina[6], Shivani Misra[2, 6*] and Guy A. Rutter[1,2,7,8*]

[1]Centre de Recherche du CHUM, and Faculty of Medicine, University of Montreal, QC, Canada

[2]Department of Metabolism, Digestion and Reproduction, Faculty of Medicine, London, UK

[3]Departments of Pediatrics, Naomi Berrie Diabetes Center, Irving Medical Center, Columbia University, New York, USA

[4]MRC Laboratory of Medical Sciences, West London, UK

[5] Genetics & Genomic Medicine Department, UCL Great Ormond Street Institute of Child Health, London, United Kingdom

[6]Department of Diabetes, Imperial College Healthcare NHS Trust, London, UK

[7]Lee Kong Chian Imperial Medical School, Nanyang Technological University, Singapore

[8]Research Institute of the McGill University Hospital Centre, Montréal, QC, Canada

Address correspondence to Prof. Guy A. Rutter, Tel 514 890-8000, ext. 27081,

guy.rutter@umontreal.ca or Dr Shivani Misra, S.misra@imperial.ac.uk

Abstract

Monogenic diabetes, formerly called Maturity-Onset Diabetes of the Young (MODY), involves single-gene mutations, typically with dominant inheritance, and has been associated with variants in 14 genes. Among these, *HNF1A* mutations are the most common, and their diagnosis allows the use of alternative therapies, including sulfonylureas. In an earlier study, we described a variant displaying recessive transmission, p.A251T (Misra, S et al, *Diabetes Care*, 2020). Initial functional studies revealed only a modest impact on protein function. We extend these earlier *in vitro* studies to demonstrate that beta-like cells derived from pluripotent stem cells from variant carriers show impaired differentiation into insulin-positive cells, whereas differentiation into alpha cells is significantly enhanced. Additionally, mutant cells showed impaired glucose-stimulated insulin secretion but partially preserved responsiveness to treatment with sulfonylureas. Our study provides proof of principle for the utility of using patient-derived stem cells as a platform to assess the pathogenicity of *HNF1A* variants, and to explore potential treatment strategies.

1. Introduction

Monogenic diabetes is a rare form of non-immune diabetes that results from mutations in a single gene, leading to impaired beta-cell function (Fajans et al., 2001). HNF1A-MODY, caused by mutations in the *HNF1A* gene, is the predominant form of the disease (McDonald & Ellard, 2013). Accurate diagnosis of HNF1A-MODY is crucial for optimising treatment strategies, such as the use of sulfonylureas, which have been shown to effectively manage glycemia in patients with a correct diagnosis (Pearson et al., 2000). Next-generation DNA sequencing is the most accurate way of detecting mutations in MODY genes. However, the identification of genetic variants of unknown significance (VUSs) presents a challenge, as their pathogenicity and impact on diabetes progression are often unknown. To better understand the pathogenicity of VUSs, well-established *in vitro* assays of HNF1A function—such as DNA binding, subcellular localisation, and transactivation capacity—are performed in commonly used immortalised cell lines (Bjørkhaug et al., 2003; Colclough et al., 2013). However, these cell lines may not fully replicate human beta-cell physiology, limiting their use in exploring potential therapeutic strategies to rescue insulin secretion.

The present study focuses on the pathogenicity of a recessive *HNF1A* VUS, the missense variant p.A251T (c.751G>A), identified in early-onset diabetes patients from the 'MY DIABETES' study (MODY in Young-Onset Diabetes in Different Ethnicities, Clinical Trial No. NCT02082132, ClinicalTrials.gov). *In vitro* functional studies (Misra et al., 2020) indicated that the *HNF1A* p.A251T variant leads to modest defects in transactivation, suggesting a partial impairment of HNF1A protein function. These findings point to a compromised ability of HNF1A to regulate target gene expression,

potentially driving beta-cell dysfunction. Despite these relatively mild defects *in vitro*, patients carrying this specific variant on both alleles can often manage their glycemic control more effectively with low-dose sulfonylurea treatment rather than with insulin (Misra et al., 2020). This therapeutic approach aligns with the characteristic HNF1A-MODY phenotype (Pearson et al., 2000). Our hypothesis is that these variants impair HNF1A function, disrupting beta-cell function and contributing to the diabetic phenotype. We generated human induced pluripotent stem cells (iPSCs) from patient fibroblasts, and subsequent differentiation into beta-like cells provided a more robust platform to closely mimic and better understand the pathogenicity of the *HNF1A* p.A251T variant.

2. Methods

The DIPS study, studying rare diabetes using iPSC, PI: Dr. Shivani Misra, was approved by Westminster Research Ethics Committee (20/LO/1071) to perform skin biopsies from probands carrying the *HNF1A* p. A251T variants.

Plasmid design

A vector containing human pancreatic *HNF1A* cDNA in a pcDNA3.1 backbone was used for all functional studies, provided by the Oxford Centre for Diabetes Endocrinology and Metabolism (Althari et al., 2020). This vector serves as *HNF1A* Wild-Type (WT) control, allowing for comparison with the *HNF1A* constructs containing variants. Additionally, the pcDNA3.1 backbone plasmid was employed as a control for “empty” vector, without genetic material or for value correction in DNA-binding activity assays. The variants used as positives controls for HNF1A impaired protein function included the MODY-

causing mutations p.P112L (Bjørkhaug et al., 2003), p.R203H (Colclough et al., 2013) and p.T260M (Glucksmann et al., 1997), and the p.E508K variant associated with an increased risk of T2D (Martagón et al., 2018) offered by the Oxford Centre for diabetes Endocrinology and Metabolism, Churchill Hospital.

Site-directed mutagenesis

To generate the *HNF1A* variants of interest p.A251T site-directed mutagenesis was performed on the *HNF1A* cDNA in the pcDNA3.1 vector using the Q5 Site-Directed Mutagenesis Kit (New England BioLabs). Site-directed mutagenesis was performed using PCR amplification with Q5 Hot Start High-Fidelity 2X Master Mix, Forward Primer, Reverse Primer, and Template *HNF1A* cDNA. The PCR amplification process used Q5 Hot Start High-Fidelity (New England Biolabs) with its specific cycling conditions consisting of an initial denaturation step at 98°C for 30 seconds, followed by 25 cycles of denaturation at 98°C for 10 seconds, annealing at a temperature range of 50-72°C for 30 seconds, and extension at 72°C for 30 seconds per kilobase of DNA. Next, PCR products were incubated with a KLD (provided with Q5 Site-Directed Mutagenesis Kit), a combination of enzymes including Kinase, Ligase, and DpnI restriction enzyme, at room temperature. The KLD mix product was transformed into NEB 5-alpha Competent E. coli cells. This was achieved by placing the KLD mix/Competent cells mixture on ice for 30 minutes, followed by a brief heat shock at 42°C for 30 seconds, and then returning it to ice. The mixture was supplemented with SOC medium (provided with Q5 Site-Directed Mutagenesis Kit) and incubated at 37°C with shaking at 250 rpm for 1 hour. Finally, the transformed cells were spread onto an ampicillin selection plate and incubated overnight at 37°C.

Plasmid isolation

Plasmids were extracted from competent *E. coli* cells using the QIAprep Spin Miniprep Kit (Qiagen), following the provided instructions. After washes and elution, the DNA was quantified using a Nanodrop 2000 spectrophotometer (ThermoScientific).

The sequence of all constructs was validated using Sanger sequencing (Primer sequence for sequencing: 5'-CCGAGCCATGGTTTCTAAACTG-3'). Reporter gene in pGL3 vector, contained HNF1A transcription factor recognition sequence next to a *Firefly* luciferase reporter gene and either the Rat Albumin promoter, pGL3-RA, or HNF4A P2 promoter, pGL3-P2, both constructs were offered by the Oxford Centre for diabetes Endocrinology and Metabolism. A reporter pRL-SV40 (Promega) containing *Renilla reniformis* luciferase gene, was used as a transfection control for all the experiments.

Cell culture and transfection

HeLa cells (Lucey et al., 2009) were cultured at 5% CO_2, at 37 °C, in T-75 cell culture flasks (Sarstedt), in DMEM (Gibco,) supplemented with 1% penicillin-streptomycin (ThermoFisher) and 10% Foetal Bovine Serum (FBS, Gibco). HeLa cells were passaged at ≥ 70% confluency. The INS1 832/3 cells (Asfari et al., 1992; Hohmeier et al., 2000) were maintained at 5% CO_2, at 37 °C, in T75 cell culture flasks, in RPMI-1640 medium (ThermoFisher) supplemented with 10% FBS, 2 mM L-glutamine brand (Sigma), 1 mM sodium pyruvate (ThermoFisher), 10 mM HEPES (Sigma), and 0.05 mM beta-mercaptoethanol (Sigma). INS1 832/3 were passaged every 4 days at ≥ 70% confluency. Both cell lines were passaged using Trypsin-EDTA Solution 1X (Sigma) at 37°C for 5 minutes. Transfections were performed using 3 μL of Lipofectamine 2000

(Thermo Fisher) with 2 μg of DNA: 0.25 μg pcDNA3.1-WT HNF1A, 0.25 μg pcDNA3.1-HNF1A variants or empty vector, 0.50 μg pGL3-RA, and 0.010 μg pRL-SV40, in 500 μL of cell-specific medium.

Transactivation assay

HeLa and INS1 832/3 were cultured in a p24-culture plate (Thermo Fisher) until they reached over 90% confluence. Cells were transiently transfected (48h) with either *HNF1A* WT or variant plasmids, along with the reporter plasmids pGL3-RA/pGL3-P2 and pRL-SV40. Following a 48-hour period of transfection, the cells were lysed using the lysis buffer provided with the Dual-Luciferase Reporter Assay (Promega Corp). A portion of the lysate was immediately used for the luciferase assay, the luciferase assay was performed following the manufacturer's instructions. The luminometer (Berthold Tube Luminometer) was programmed to perform two measurements with delays in capturing, first the luminescence signals of *Firefly* Luciferase (using LAR II solution provided with the kit) and second, the *Renilla* Luciferase (using Stop & Glo Reagent). The normalised ratio of activity was calculated for each variant "Experimental Reporter Activity/Control Reporter Activity" and then averaged for all replicates readings. Luciferase measurements were given in percentage activity compared to WT.

DNA-binding assay

HeLa cells were transiently transfected (24h), with WT or *HNF1A* variant plasmids. Nuclear protein extract was obtained using the nuclear extraction kit (Abcam). The nuclear extract was then incubated with a biotin-labelled oligonucleotide containing the target HNF1A DNA binding sequence. DNA-binding of HNF1A was determined using

DNA-Protein Binding Assay Kit (Colorimetric) (Abcam) according to the manufacturer's guidelines. The resulting oligo-protein complex was captured on the assay microwell and detected using a HNF1A primary antibody (Santa Cruz) and Horseradish Peroxidase (HRP) secondary antibodies (GE Healthcare). Quantitative measurements of the colorimetric reactions were performed using Microplate Reader (BMG reader). The analysis involved calculating the binding activity using the formula: "Binding Activity = (Sample OD – Blank OD) x sample dilution".

Subcellular localisation

INS1 832/3 cells were transiently transfected (24h), with WT or *HNF1A* variant plasmids. The HNF1A subcellular localisation of WT and *HNF1A* variants was assessed using a primary 6x-His Tag Monoclonal Antibody (ThermoFisher) followed by a secondary antibody, Alexa Fluor 488 (ThermoFisher). The slides were mounted using ProLong Diamond Antifade Mounting solution with DAPI (Invitrogen) and examined using the Eclipse T-I Microscope with a spinning disc confocal system (Nikon), x40, oil immersion. A minimum of 30 cells were analysed to determine the presence of staining in the nucleus only and in both the nucleus and cytoplasm, 3 experiments were performed using 3 biological replicates for each variant and WT.

Collection of skin punch biopsy and culture of fibroblasts

Using a biopsy punch, 4-mm-diameter epidermal biopsies were obtained. Skin sample were cut into 5-15 smaller sections in a T75 flask and cultured at 37 °C with 5% CO2 in Dulbecco's Modified Eagle's Medium (DMEM; Thermo Fisher) supplemented with 15% Foetal Bovine Serum (FBS; Thermo Fisher) and Antibiotic-Antimycotic cocktail (Gibco).

At day 15, fibroblasts outgrown from the skin biopsies. Fibroblasts were passaged at 70% confluency using Trypsin-Edta solution 1x (Sigma) and seeded at a ratio 1:2 to 1:5 depending on the morphology and density of cells.

Generation of iPSCs using plasmids episomal vectors

Four days before transfection, fibroblasts were seeded onto a T75 flask so that they would reach between 80-90% confluency on the day of transfection. A minimum of $3x10^6$ fibroblast cells were electroporated (1650V, 10ms, 3 pulses) with 3ug of three 3 reprogramming plasmids containing the episomal factors Oct4, Sox2, Klf4, Lin28, and L-Myc (OSKM): pCXLE-hSK (Addgene), pCXLE-hUL (Addgene) and pCXLE-hOCT3/4-shp53-F (Addgene) (Takahashi & Yamanaka, 2016). Fibroblasts were resuspended in pre-warmed fibroblast medium containing DMEM, supplemented with 15% FBS, 10 mM Y-27632 (ROCK inhibitor, Stem Cell Technology), and 4 ng/mL Heat Stable Recombinant Human bFGF (Thermo Fisher). From days 1 to 15 post-transfection, the media was switched to supplemented N2B27 Medium containing DMEM/High Glucose plus N2 (Thermo Scientific) and B27 without Vitamin A (Thermo Fisher), supplemented with CHALP molecules: 0.5 µM PD0325901 (MEK Inhibitor, Sigma), 3 µM CHIR99021 (GSK3beta-inhibitor, Sigma), 0.5 µM A-83-01 (TGF-beta/Activin/Nodal receptor inhibitor, Reprocell), 10 ng/mL hLIF (STEMCELL Technologies), 10 µM HA-100 (Santa Cruz) and 100 ng/mL bFGF. The N2B27 Medium with CHALP was replaced every 48 hours. On day 15 post-transfection, the supplement N2B27 Medium was replaced with Essential 8 Medium (Thermo Fisher) or StemFlex (SF, Thermo Fisher) for human stem cell culture and changed every 24 hours. Between days 15 to 30, iPSC-like colonies start appearing. Between days 21 to 40 post-transfection, colonies are of

sufficient size to be manually picked and expanded in Getrex-coated 24-well plates (Thermo Fisher) for 10 passages.

iPSCs culture

iPSCs were cultured in StemFlex (Thermo Fisher) on 1% Geltrex-coated six-well plates (Thermo Fisher) and passaged using TrypLE Express (Thermo Fisher) at a 1:10 to 1:50 ratio, when cells reached 80-90% confluence. After passages, iPSCs were resuspended in medium containing 1 μL/mL of 10 mM ROCK inhibitor (Y-27632, STEMCELL Technologies) for 24 hours. The medium was then replaced with SF without ROCK inhibitor, and refreshed every other day until the next passage. Cells were maintained in a 37°C, 5% CO□ humidified incubator.

Generation of beta-like cells by directed differentiation

iPSCs carrying the *HNF1A* p.A251T variant were differentiated into beta-like cells (Cherkaoui et al., 2024; Sui et al., 2018, 2021) and compared with iPSCs (1159) derived from a healthy donor. iPSCs were initially seeded in SF medium (Thermo Fisher) for 2 hours to achieve 100% confluence (1.8–2.1 x10^6 cells per well of a 6-well plate) on a Geltrex-coated 6-well plate (Thermo Fisher). The SF medium was then replaced with definitive endoderm basal medium supplemented with components A and B from the definitive endoderm kit (Stem Cell Technologies) in a 1:100 ratio and incubated for 24 hours at 37°C in 5% CO□. On day 2, the medium was replaced with fresh definitive endoderm basal media supplemented with component B (1:100 ratio) for 36 hours, and then replaced with fresh medium for an additional 24 hours. From days 4 to 6, the cells were cultured in primitive gut tube medium (RPMI 1640, GlutaMAX, 1% penicillin-

streptomycin, 1% B-27, 50 ng/mL FGF7), followed by posterior foregut medium from days 6 to 8 (DMEM, GlutaMAX, 1% penicillin-streptomycin, 1% B-27, 0.25 μM KAAD-cyclopamine, 2 μM retinoic acid, 0.25 μM LDN193189). From days 8 to 12, cells were cultured in pancreatic progenitor medium (DMEM, GlutaMAX, 1% penicillin-streptomycin, 1% B-27, 50 ng/mL EGF, 25 ng/mL FGF7). At day 12, cells were detached using TrypLE, resuspended in cluster medium (DMEM, GlutaMAX, 1% penicillin-streptomycin, 1% B-27, 1 μM RepSox, 25 ng/mL FGF7, 10 μg/mL heparin, 10 μM Y-27632), and transferred to AggreWell 400 microwell plates (STEMCELL Technologies) for 24 hours. On day 13, clusters were transferred to low-adhesion plates, and pancreatic endocrine progenitor medium (RPMI, GlutaMAX, 1% penicillin-streptomycin, 1% B-27, 1 μM thyroid hormone (T3), 10 μM RepSox, 10 μM zinc sulfate, 100 nM gamma-secretase inhibitor, 10 μM Y-27632) was added. Medium was changed daily until day 15, at which point the clusters were collected and incubated in fresh pancreatic endocrine progenitor medium supplemented with 1 μM aphidicolin until day 20. From days 20 to 27, the cells were cultured in pancreatic beta-cell stage medium (RPMI, GlutaMAX, 1% penicillin-streptomycin, 1% B-27, 10% FBS, 10 μM Ri). Beta-like cells were harvested and ready for analysis on day 25.

Immunofluorescence staining

At day 25, 10-15 clusters were collected, fixed with 4% paraformaldehyde for 15 minutes, and washed with PBS (Thermo Fisher). Clusters were incubated in 30% sucrose overnight at 4°C, embedded in optimal cutting temperature (O.C.T.) compound, and frozen. Cryosections (5-10 μm) were prepared, mounted onto SuperFrost Plus slides (Thermo Fisher), and stored at -80°C. Sections were rehydrated in PBS for 15 minutes,

followed by methanol incubation at −20°C for 10 minutes. After washing, sections were blocked with 2% normal donkey serum in PBS for 1 hour at room temperature, then incubated overnight at 4°C with primary antibodies against insulin (Dako, 1:50), glucagon (Sigma, 1:5000), NKX6.1 (Novus Biologicals, 1:2000), and PDX1 (Abcam, 1:1000). After washing, slides were incubated with appropriate secondary antibodies (Alexa Fluor 488, 561, 568, 647) for 1 hour at room temperature. Slides were mounted with ProLong Diamond Antifade Mounting medium with DAPI (Invitrogen) and visualised using a STELLARIS 8 Inverted Confocal Microscope (Leica), 40x oil immersion objective.

Glucose-Stimulated Insulin Secretion (GSIS) assay

KREBS solutions (118 mM NaCl, 4.7 mM KCl, 1.2 mM $MgSO_4$, 1.2 mM KH_2PO_4, 2.5 mM $CaCl_2$, 25 mM $NaHCO_3$, 10 mM HEPES) were prepared with low glucose (3.3 mM) or high glucose (16.7 mM) and bubbled with CO_2 to adjust the pH to 7.2. Beta-like cell clusters (10–15 per sample) were first incubated in low-glucose KREBS solution at 37°C for 1 hour, followed by incubation in high-glucose KREBS solution for 30 minutes. Additional treatments included Exendin-4 (100nM, 30 minutes), glibenclamide (1 μM, 30 minutes), KCl (30 minutes). After incubation, 200 μL of the supernatant from each condition was collected, stored at -80°C, or used directly for insulin quantification. Insulin levels were measured using an ultra-sensitive HTRF insulin assay (Cisbio), according to the manufacturer’s instructions.

Quantification of total Insulin

After the GSIS assay, islet clusters were lysed in acid-ethanol solution (50 µL ultrapure water and 150 µL acid ethanol) and stored overnight at 4°C. The following day, samples were vortexed, sonicated for 10 seconds, and centrifuged at 10,000×g for 10 minutes. DNA concentration was measured using a nanodrop spectrophotometer (A260 nm), and insulin levels were normalised to DNA content.

Statistical analysis

All analyses were conducted using GraphPad Prism 9 software. The Shapiro test (Shapiro and Wilk, 1965) was used to assess the normality of the data. Mean ± SEM was reported for normally distributed data, while median with interquartile range (IQR) was reported for data that did not follow a normal distribution. Unpaired Student's two-tailed t-test was used for comparing two groups when the data met parametric assumptions. In cases where the data did not meet parametric assumptions, the Mann-Whitney U test was employed for two-group comparisons. For parametric comparisons involving multiple groups, two-way ANOVA was used. Statistical significance was considered when p-value were equal to or less than 0.05 (*), 0.01 (**), 0.001 (***), or 0.0001 (****)

3. Results

In vitro functional assessment of the *HNF1A* p.A251T variant

To assess the pathogenicity of the p.A251T variant, we performed functional analyses using well-established *in vitro* assays (Misra et al., 2020), including luciferase reporter assays to measure transcriptional activity of HNF1A, DNA-binding activity assay and subcellular localisation. These assays were performed in HeLa (immortalised human

cervical carcinoma cells) and INS-1 832/3 (rat insulinoma cells). The p.A251T variant was generated via site-directed mutagenesis of human pancreatic *HNF1A* cDNA in the pcDNA3.1A vector, and the construct was validated by Sanger sequencing, confirming the c.751G>A mutation.

In HeLa cells, the p.A251T variant exhibited no significant effect on transactivation, retaining 86% of WT activity (Figure 1A; ns). Similarly, in INS-1 832/3 cells, the p.A251T variant displayed activity comparable to WT (Figure 1A; 101% of WT, ns). These findings suggest that the p.A251T variant has a minimal impact on transactivation *in vitro*, consistent with previous reports (Misra et al., 2020). We conducted additional experiments to evaluate the transactivation activity of the *HNF1A* p.A251T variant, using the same approach as previous experiments, but including a comparison with the MODY-causing mutations p.P112L (Bjørkhaug et al., 2003), p.R203H (Colclough et al., 2013), and p.T260M (Glucksmann et al., 1997). In HeLa cells, the p.P112L variant displayed 30% of WT activity (Supplementary Figure 1B, **p = 0.005), while p.T260M exhibited 34% of WT activity (Supplementary Figure 1B, *p = 0.01). The p.A251T variant showed no significant change, maintaining 62% of WT activity (Supplementary Figure 1B, HeLa, ns). In INS-1 832/3 cells, p.T260M demonstrated 41% of WT activity (Supplementary Figure 1A, *p = 0.05), and p.P112L showed 32% of WT activity (Supplementary Figure 1A, *p = 0.03). In contrast, p.A251T displayed similar activity to WT, with 77% of WT levels (Supplementary Figure 1A, ns).

The p.A251T variant is located within the DNA-binding domain of the HNF1A protein. To evaluate its effect on DNA binding, we conducted DNA-binding assays, which

revealed a modest decrease in binding activity for the p.A251T variant (62% of WT, ns, Figure 1B), though this difference was not statistically significant. Western blot analysis confirmed that there were no significant differences in protein expression levels between the p.A251T variant and WT HNF1A (Supplementary Information, Figure 2A-B), indicating that the observed transactivation activity and DNA-binding were not due to differences in protein expression.

Analysis of subcellular localisation was performed to assess the effect of the p.A251T recessive variant on the nuclear localisation of HNF1A. INS-1 832/3 cells were transiently transfected with 6xHis-tagged WT or p.A251T HNF1A. The nuclear-to-total fluorescence ratio was quantified using confocal microscopy, measuring the relative distribution of HNF1A in the nuclear versus cytoplasmic compartments. Our results show that the nuclear-to-total fluorescence ratio of 6xHis-tagged HNF1A in INS-1 cells expressing the p.A251T variant was significantly lower than that observed in WT HNF1A-transfected cells, with WT showing 88% nuclear accumulation compared to 81% for the p.A251T variant (Figure 1C, **p=0.007). These findings suggest that the p.A251T variant impacts the nuclear import, retention, or overall subcellular localisation of the HNF1A protein.

Generation and validation of iPSCs from a proband homozygous for the *HNF1A* p.A251T variant

The p.A251T variant exhibits minimal functional effects *in vitro*, showing only a tendency towards reduction in DNA binding compared to WT and a modest decrease in nuclear accumulation of the HNF1A protein. However, these impairments are in contrast

to the clinical presentation of the homozygous carriers, which exhibit features similar to classical heterozygous HNF1A-MODY.

Functional assays were conducted in immortalised cell lines overexpressing the *HNF1A* p.A251T variant, though these models do not fully replicate the pathophysiology of MODY. To gain deeper insight into the pathogenicity of the *HNF1A* p.A251T variant, we generated iPSCs from a proband homozygous for the *HNF1A* p.A251T mutation. Skin biopsies were collected from the proband, and fibroblasts were reprogrammed into iPSCs using a selective culture method and reprogramming factors Oct4, Sox2, Nanog, Lin28, L-Myc, and Klf4 (Takahashi & Yamanaka, 2016) (Figure 2). The DIPS study, studying rare diabetes using iPSC, PI: Dr. Shivani Misra, was approved by Westminster Research Ethics Committee (20/LO/1071) to perform skin biopsies from probands carrying the HNF1A p. A251T variants.

To validate the iPSCs, a karyotype analysis was performed on the iPSC clones, confirming a normal karyotype with 46 chromosomes, including two X chromosomes, consistent with the donor's female sex (Figure 2E). To assess the pluripotency of the iPSC clones, alkaline phosphatase (AP) activity was evaluated using a colorimetric assay. Only clones with strong alkaline phosphatase (AP) activity were selected. Colonies were manually counted after passage 10 to ensure that only those exhibiting robust AP positivity (as shown in Supplementary Figure 3) were retained.

Additionally, we assessed the relative expression of OCT-4 (Figure 2B-C). The iPSCs derived from the proband carrying the *HNF1A* p.A251T variant exhibited a mean OCT-4 expression of 98.9% ± 0.6% (n = 15), in contrast to fibroblasts from the same proband,

which did not express OCT-4. These results confirm that the A251T iPSCs retained the key hallmarks of pluripotency.

Lower insulin secretion in A251T beta-like cells

A251T iPSCs were directed to differentiate into beta-like cells (according to Cherkaoui et al., 2024; Sui et al., 2018, 2021). This differentiation protocol is a modified version of the method established by Sui et al. (2018), with the addition of the DNA polymerase alpha inhibitor aphidicolin from days 15 to 30. This treatment was incorporated to enhance the yield of insulin-positive cells, as demonstrated in previous studies. (Sui et al., 2021). *HNF1A* dominant mutations have been implicated in the impairment of glucose-stimulated insulin secretion, as demonstrated in beta-like cells derived from *HNF1A* knockout (KO) hESCs (Cardenas-Diaz et al., 2019; González et al., 2022). Given that the p.A251T *HNF1A* recessive variant was associated with reduced C-peptide levels in the proband (Misra et al., 2020), we aimed to investigate whether this variant produces a comparable phenotype *in vitro* using an A251T iPSC-derived beta-cells. Our investigation focused on evaluating the beta-cell response to glucose stimulation at both low and high concentrations, as well as to various secretagogues. These included sulfonylureas, which has been observed to affect insulin secretion in clinical cases (Misra et al., 2020), and the GLP-1 agonist Exendin-4. In all analyses, beta-like cells with the A251T variant were compared to the control line 1159, which was derived from a healthy donor (provided by the Stem Cell Initiative at Columbia University).

The results revealed no significant difference in insulin secretion at baseline glucose concentration (3.3 mM, Figure 3) between A251T variant and control cells. However,

when challenged with a higher glucose concentration (16.7 mM, Figure 3), the A251T variant beta-like cells exhibited significantly reduced insulin secretion compared to control 1159 cells (p=0.003, n = 9, Figure 3). Specifically, the A251T beta-like cells secreted 0.05% of insulin (normalised to total insulin content) compared to 0.20% in the control 1159 cells. Similarly, under high glucose conditions combined with GLP-1 receptor agonist Exendin-4 (16.7 mM + Ex-4, Figure 3) or the sulfonylurea glibenclamide (16.7 mM + GLB, Figure 3), the A251T variant beta-like cells exhibited significantly lower insulin secretion (p =0.0008, n = 9; p = 0.01, n = 9, respectively, Figure 3) compared to the control 1159 beta-like cells. Specifically, insulin secretion was 0.12% of total insulin in the A251T cells versus 0.31% in the control cells with Exendin-4, and 0.21% versus 0.34% with GLB (Figure 3). Under conditions that mimic KATP channel closure-mediated membrane depolarisation (3.3 mM glucose + KCl, Figure 3), the A251T beta-like cells also showed significantly lower insulin secretion compared to the 1159 control cells (0.31% vs. 0.48%, p = 0.001, n = 9, Figure 3).

Glibenclamide treatment resulted in significantly higher insulin secretion compared to high glucose alone in the A251T cells (p=0.002). Despite this improvement in insulin secretion with glibenclamide treatment in A251T cells compared to high glucose alone, insulin release remained significantly lower than in control cells treated with the same secretagogues (p = 0.01, Figure 3), suggesting a persistent defect in secretion that could not be fully rescued.

Reduced insulin expression in A251T iPSC-derived beta-like cells

A marked reduction in insulin expression was observed in beta-like cells derived from A251T iPSCs compared to control 1159 cells. Insulin-positive cells comprised 31.2 ± 1.2% of the total cells per cluster in the A251T cluster, compared to 42.4 ± 3.6% in the control 1159 cell cluster ($p = 0.006$, $n = 15$). The expression levels of key beta-cell markers NKX6.1 and PDX1 did not differ significantly between the A251T and control clusters. The relative expression of NKX6.1 was 21.1 ± 1.6% in A251T clusters and 24.8 ± 2.2% in control clusters ($p = 0.2$, $n = 15$), while PDX1 expression was 34.7 ± 3.5% in A251T clusters and 40.7 ± 6.2% in controls ($p = 0.4$, $n = 9$). In addition, there was no significant difference in the proportion of cells co-expressing insulin and NKX6.1 (INS+/NKX6.1+) between A251T islet-like clusters (11.5%, IQR 10.8-19.5, $n = 9$) and control clusters (16%, IQR 8.3-28.0, $n = 9$, $p > 0.9$, Mann-Whitney test).

Although the A251T variant did not appear to affect the expression of critical beta-cell transcription factors such as NKX6.1 and PDX1, the significant reduction in insulin expression suggests that the p.A251T variant may impair insulin production or processing at later stages of differentiation. It is possible that the A251T variant affects other beta-cell transcription factors or regulatory proteins, which were not specifically examined in this study.

Enhanced α-cell differentiation in A251T iPSC-derived clusters

Differentiated cell clusters derived from iPSCs carrying the A251T variant contained a heterogeneous population of pancreatic endocrine cells, including both beta-like cells (insulin-secreting) and α-like cells (glucagon-secreting). The A251T clusters exhibited a higher proportion of glucagon-positive cells, with 19.4% ± 2.2% of total cells per cluster,

compared to 13.6% ± 1.4% in the control 1159 clusters ($p = 0.04$, $n = 9$). These results suggest that the p.A251T variant may drive a differentiation shift, favoring the α-cell (glucagon-secreting) lineage during the later stages of pancreatic endocrine cell development.

4. Discussion

This study explores the pathogenic mechanisms underlying the recessive *HNF1A* p.A251T variant and its contribution to the development of MODY. Through functional analyses in HeLa and INS-1 cell lines, we assessed the impact of the p.A251T variant on HNF1A transcriptional activity, DNA binding, and subcellular localisation. While the p.A251T variant exhibited a modest reduction in DNA binding capacity, it did not significantly affect HNF1A transcriptional activity. These findings suggest that the p.A251T variant exerts a milder functional impact compared to dominant pathogenic variants such as p.P112L and p.T260M, which are known to severely reduce HNF1A transcriptional activity *in vitro* (Figure 1 A-B, Supplementary informations) (Najmi et al., 2017).

The nuclear localisation of the p.A251T variant was significantly reduced compared to WT HNF1A. However, this decrease was substantially less pronounced than the impairment observed with the MODY variant p.Q466*, used as a control for subcellular localisation defects, which shows near-total cytosolic retention (approximately 15% nuclear accumulation, Najmi et al., 2017). These finds thus align with the recessive impact of the p.A251T variant on diabetes risk.

While the above results offer valuable insights, they also underscore the limitations of using immortalised cell lines and overexpression systems for studying subtle, recessive variants (Moriya, 2015; Pan et al., 2009; Prelich, 2012). Such models often fail to replicate the complex biological context and tissue-specific dynamics of human beta-cells, which are critical for accurately modeling diseases like MODY (Kachamakova-Trojanowska et al., 2019).

To address these limitations, we turned to a physiologically relevant model of iPSC-derived beta-cells, generated from the proband's cells. iPSC technology provides a powerful platform to investigate genetic variants in a disease-relevant context, as it allows for the generation of human beta-like cells that closely resemble native pancreatic beta-cells in both function and phenotype. This approach not only enables the study of beta-cell dysfunction in a controlled *in vitro* system but also offers a more accurate study of the molecular and cellular impacts associated with MODY.

Our results demonstrate that iPSC-derived beta-cells carrying the p.A251T *HNF1A* variant exhibit impaired insulin secretion in response to high glucose levels, a hallmark of HNF1A-MODY. This defect was further corroborated by a reduction in insulin expression in the p.A251T cells, closely mirroring the clinical phenotype observed in patients with *HNF1A* mutations. Importantly, when exposed to sulfonylurea (GLB), the A251T-derived beta-like cells showed a partial restoration of insulin secretion, recapitulating the clinical response of HNF1A-MODY patients to sulfonylurea therapy (Pearson et al., 2000). This observation suggests that the p.A251T variant disrupts beta-cell function in a manner consistent with the known therapeutic response in MODY

patients, providing strong evidence for the pathogenicity of this variant (Misra et al., 2020).

Moreover, our study revealed a significant shift in the differentiation trajectory of the A251T iPSC-derived clusters, with an increased proportion of glucagon-positive α-like cells. This shift toward α-cell differentiation suggests a potential alteration in HNF1A role during pancreatic endocrine cell differentiation. These findings are also consistent with previous data from knockout models, which show that *HNF1A* KO hESCs lead to an increase in α-cell-like populations in derived clusters (Cardenas-Diaz et al., 2019; González et al., 2022).

While traditionally considered a key regulator of beta-cell identity, our findings highlight that HNF1A may also play a broader role in maintaining the balance between insulin-secreting beta-cells and glucagon-secreting α-cells. The shift toward α-cell differentiation could impact glucose regulation in individuals with *HNF1A* mutations, potentially worsening the pathophysiology of MODY by disrupting the balance between insulin and glucagon secretion.

5. Limitation of the study

An important limitation of this study is the absence of an isogenic control, which prevents us from definitively attributing the marked differences observed between the A251T beta-like cells and the 1159 control cells to the A251T variant itself (e.g. insulin secretion, reduces insulin relative expression).

6. Conclusion

This study provides insights into the pathogenic mechanisms of the *HNF1A* p.A251T variant in the context of MODY. By using iPSC-derived beta-cells as a proof-of-principle model, we have demonstrated the utility of this approach in uncovering subtle defects in beta-cell function and differentiation that might otherwise be missed in conventional models.

7. Acknowledgments

We acknowledge support from the Facility for Imaging by Light Microscopy (FILM) at Imperial College London, which is part-supported by funding from the Wellcome Trust (grant 104931/Z/14/Z) and BBSRC (grant BB/L015129/1).

G.A.R. was supported by a Wellcome Trust Investigator Award (WT212625/Z/18/Z), MRC Programme grant (MR/R022259/1), Diabetes UK (BDA 16/0005485) and NIH-NIDDK (R01DK135268, 1R01DK139630-01A1) project grants, a CIHR-JDRF Team grant (CIHR-IRSC TDP-186358 and JDRF 4-SRA-2023-1182-S-N), CRCHUM start-up funds, and an Innovation Canada John R. Evans Leader Award (CFI 42649).

Conflict of interest.

GAR has received grant funding from and is a consultant for Sun Pharmaceuticals Inc.

No other author declares a competing interest.

8. References

Althari, S., Najmi, L. A., Bennett, A. J., Aukrust, I., Rundle, J. K., Colclough, K., Molnes, J., Kaci, A., Nawaz, S., van der Lugt, T., Hassanali, N., Mahajan, A., Molven, A., Ellard, S., McCarthy, M. I., Bjørkhaug, L., Njølstad, P. R., & Gloyn, A. L. (2020). Unsupervised Clustering of Missense Variants in HNF1A Using Multidimensional Functional Data Aids Clinical Interpretation. *American Journal of Human Genetics*, *107*(4), 670–682. https://doi.org/10.1016/j.ajhg.2020.08.016

Asfari, M., Janjic, D., Meda, P., Li, G., Halban, P. A., & Wollheim, C. B. (1992). Establishment of 2-mercaptoethanol-dependent differentiated insulin-secreting cell lines. *Endocrinology*, *130*(1), 167–178. https://doi.org/10.1210/endo.130.1.1370150

Bjørkhaug, L., Sagen, J. V., Thorsby, P., Søvik, O., Molven, A., & Njølstad, P. R. (2003). Hepatocyte nuclear factor-1 alpha gene mutations and diabetes in Norway. *The Journal of Clinical Endocrinology and Metabolism*, *88*(2), 920–931. https://doi.org/10.1210/jc.2002-020945

Cardenas-Diaz, F. L., Osorio-Quintero, C., Diaz-Miranda, M. A., Kishore, S., Leavens, K., Jobaliya, C., Stanescu, D., Ortiz-Gonzalez, X., Yoon, C., Chen, C. S., Haliyur, R., Brissova, M., Powers, A. C., French, D. L., & Gadue, P. (2019). Modeling Monogenic Diabetes using Human ESCs Reveals Developmental and Metabolic Deficiencies Caused by Mutations in HNF1A. *Cell Stem Cell*, *25*(2), 273-289.e5. https://doi.org/10.1016/j.stem.2019.07.007

Cherkaoui, I., Du, Q., Egli, D., Misra, S., & Rutter, G. A. (2024). Optimized Protocol for Generating Functional Pancreatic Insulin-secreting Cells from Human Pluripotent Stem Cells. *Journal of Visualized Experiments: JoVE*, *204*. https://doi.org/10.3791/65530

Colclough, K., Bellanne-Chantelot, C., Saint-Martin, C., Flanagan, S. E., & Ellard, S. (2013). Mutations in the genes encoding the transcription factors hepatocyte nuclear factor 1 alpha and 4 alpha in maturity-onset diabetes of the young and hyperinsulinemic hypoglycemia. *Human Mutation*, *34*(5), 669–685. https://doi.org/10.1002/humu.22279

Fajans, S. S., Bell, G. I., & Polonsky, K. S. (2001). Molecular mechanisms and clinical pathophysiology of maturity-onset diabetes of the young. *The New England Journal of Medicine*, *345*(13), 971–980. https://doi.org/10.1056/NEJMra002168

Glucksmann, M. A., Lehto, M., Tayber, O., Scotti, S., Berkemeier, L., Pulido, J. C., Wu, Y., Nir, W. J., Fang, L., Markel, P., Munnelly, K. D., Goranson, J., Orho, M., Young, B. M., Whitacre, J. L., McMenimen, C., Wantman, M., Tuomi, T., Warram, J., … Thomas, J. D. (1997). Novel mutations and a mutational hotspot in the MODY3 gene. *Diabetes*, *46*(6), 1081–1086. https://doi.org/10.2337/diab.46.6.1081

González, B. J., Zhao, H., Niu, J., Williams, D. J., Lee, J., Goulbourne, C. N., Xing, Y., Wang, Y., Oberholzer, J., Blumenkrantz, M. H., Chen, X., LeDuc, C. A., Chung, W. K., Colecraft, H. M., Gromada, J., Shen, Y., Goland, R. S., Leibel, R. L., & Egli, D. (2022). Reduced calcium levels and accumulation of abnormal insulin granules in stem cell models of HNF1A deficiency. *Communications Biology*, *5*(1), 779. https://doi.org/10.1038/s42003-022-03696-z

Hohmeier, H. E., Mulder, H., Chen, G., Henkel-Rieger, R., Prentki, M., & Newgard, C. B. (2000). Isolation of INS-1-derived cell lines with robust ATP-sensitive K+ channel-dependent and -independent glucose-stimulated insulin secretion. *Diabetes*, *49*(3), 424–430. https://doi.org/10.2337/diabetes.49.3.424

Kachamakova-Trojanowska, N., Stepniewski, J., & Dulak, J. (2019). Human iPSCs-Derived Endothelial Cells with Mutation in HNF1A as a Model of Maturity-Onset Diabetes of the Young. *Cells*, *8*(11), 1440. https://doi.org/10.3390/cells8111440

Lucey, B. P., Nelson-Rees, W. A., & Hutchins, G. M. (2009). Henrietta Lacks, HeLa Cells, and Cell Culture Contamination. *Archives of Pathology & Laboratory Medicine*, *133*(9), 1463–1467. https://doi.org/10.5858/133.9.1463

Martagón, A. J., Bello-Chavolla, O. Y., Arellano-Campos, O., Almeda-Valdés, P., Walford, G. A., Cruz-Bautista, I., Gómez-Velasco, D. V., Mehta, R., Muñoz-Hernández, L., Sevilla-González, M., Viveros-Ruiz, T. L., Ordoñez-Sánchez, M. L., Rodríguez-Guillen, R., Florez, J. C., Tusié-Luna, M. T., Aguilar-Salinas, C. A., & Slim Initiative in Genomic Medicine for the Americas (SIGMA) Type 2 Diabetes Consortium. (2018). Mexican Carriers of the HNF1A p.E508K Variant Do Not Experience an Enhanced Response to Sulfonylureas. *Diabetes Care*, *41*(8), 1726–1731. https://doi.org/10.2337/dc18-0384

McDonald, T. J., & Ellard, S. (2013). Maturity onset diabetes of the young: Identification and diagnosis. *Annals of Clinical Biochemistry*, *50*(Pt 5), 403–415. https://doi.org/10.1177/0004563213483458

Misra, S., Hassanali, N., Bennett, A. J., Juszczak, A., Caswell, R., Colclough, K., Valabhji, J., Ellard, S., Oliver, N. S., & Gloyn, A. L. (2020). Homozygous Hypomorphic HNF1A Alleles Are a Novel Cause of Young-Onset Diabetes and Result in Sulfonylurea-Sensitive Diabetes. *Diabetes Care*, *43*(4), 909–912. https://doi.org/10.2337/dc19-1843

Moriya, H. (2015). Quantitative nature of overexpression experiments. *Molecular Biology of the Cell*, *26*(22), 3932–3939. https://doi.org/10.1091/mbc.E15-07-0512

Najmi, L. A., Aukrust, I., Flannick, J., Molnes, J., Burtt, N., Molven, A., Groop, L., Altshuler, D., Johansson, S., Bjørkhaug, L., & Njølstad, P. R. (2017). Functional Investigations of HNF1A Identify Rare Variants as Risk Factors for Type 2 Diabetes in the General Population. *Diabetes*, *66*(2), 335–346. https://doi.org/10.2337/db16-0460

Pan, C., Kumar, C., Bohl, S., Klingmueller, U., & Mann, M. (2009). Comparative Proteomic Phenotyping of Cell Lines and Primary Cells to Assess Preservation of Cell Type-specific Functions. *Molecular & Cellular Proteomics: MCP*, *8*(3), 443–450. https://doi.org/10.1074/mcp.M800258-MCP200

Pearson, E. R., Liddell, W. G., Shepherd, M., Corrall, R. J., & Hattersley, A. T. (2000). Sensitivity to sulphonylureas in patients with hepatocyte nuclear factor-1alpha gene mutations: Evidence for pharmacogenetics in diabetes. *Diabetic Medicine: A Journal of the British Diabetic Association*, *17*(7), 543–545. https://doi.org/10.1046/j.1464-5491.2000.00305.x

Prelich, G. (2012). Gene Overexpression: Uses, Mechanisms, and Interpretation. *Genetics*, *190*(3), 841–854. https://doi.org/10.1534/genetics.111.136911

Sui, L., Leibel, R. L., & Egli, D. (2018). Pancreatic Beta Cell Differentiation From Human Pluripotent Stem Cells. *Current Protocols in Human Genetics*, *99*(1). https://doi.org/10.1002/cphg.68

Sui, L., Xin, Y., Du, Q., Georgieva, D., Diedenhofen, G., Haataja, L., Su, Q., Zuccaro, M. V., Kim, J., Fu, J., Xing, Y., He, Y., Baum, D., Goland, R. S., Wang, Y., Oberholzer, J., Barbetti, F., Arvan, P., Kleiner, S., & Egli, D. (2021). Reduced replication fork speed promotes pancreatic endocrine differentiation and controls graft size. *JCI Insight*, *6*(5), 141553. https://doi.org/10.1172/jci.insight.141553

Takahashi, K., & Yamanaka, S. (2016). A decade of transcription factor-mediated reprogramming to pluripotency. *Nature Reviews. Molecular Cell Biology*, *17*(3), 183–193. https://doi.org/10.1038/nrm.2016.8

Urakami, T. (2019). Maturity-onset diabetes of the young (MODY): Current perspectives on diagnosis and treatment. *Diabetes, Metabolic Syndrome and Obesity: Targets and Therapy*, *12*, 1047–1056. https://doi.org/10.2147/DMSO.S179793

9. Figure legend

Figure 1: Assessment of functional impact of *HNF1A* p.A251T variant in HeLa and INS-1 832/3 Cells. A: HeLa and INS-1 832/3 cells were transiently transfected with WT or variant HNF1A, or empty pcDNA3.1 vector, along with reporter plasmids pGL3-RA and pRL-SV40. Luciferase activity is shown as a percentage of WT. Data are the mean of 27 readings. B: DNA-protein binding activity was measured in HeLa cells transfected with WT or variant *HNF1A* for 24 hours using a biotin-labelled DNA-binding assay. Data are normalised to WT and corrected to the empty vector control. Each bar represents the mean of 9 measurements. C: The subcellular localisation of HNF1A protein variants was analysed in INS-1 cells. The percentage of cells showing nuclear localisation of each variant, normalised to WT, was quantified from a minimum of 30 cells per condition.

Figure 2: Reprogramming and characterisation of iPSC carrying p.A251T *HNF1A* variant . A: Overview of the iPSC reprogramming protocol. Somatic fibroblasts were transfected with episomal reprogramming vectors (Takahashi & Yamanaka, 2016) at day 4. After

transfection, cells were cultured in N2B27 media with bFGF for 14 days. Media was then switched to stem cell conditions, and colonies were picked around day 21 for further analysis. B: Confocal microscopy images showing OCT4 expression in reprogrammed iPSC colonies. Cells were stained with DAPI (blue, 405 nm) to label nuclei and OCT4 (green, 488 nm) to assess pluripotency. Imaging was performed using the Leica Stellaris 8 Confocal Microscope. Co-localisation of DAPI and OCT4 indicates pluripotency. C: Quantification of OCT4-positive cells. OCT4-positive cells were identified by co-localisation with DAPI and quantified using an automated macro. The graph shows the percentage of OCT4-positive cells relative to total cells in the colonies. D: Morphological changes during the differentiation process observed under brightfield microscopy. Day 1: Fibroblast-like cells (top left). Day 12: Intermediate cell morphology (top right). Day 15: iPSC-like colony formation. Day 18: Growth phase, ready for picking. Arrows indicate changes in cell morphology over time. Scale bar = 100 µm. E: Karyotyping analysis of selected iPSC clones. G-banding of chromosomes revealed a normal karyotype with 46 chromosomes, including two X chromosomes, consistent with the donor's female sex.

Figure 3: Glucose- and secretagogue-induced insulin secretion in A251T beta-like cells

This figure presents the percentage of insulin secretion relative to total insulin content, measured under various conditions: baseline glucose concentration (3.3 mM), high glucose stimulation (16.7 mM), high glucose with Exendin-4 (Ex-4, a GLP-1 receptor agonist) (16.7 + Ex-4), high glucose with Glibenclamide (GLB, a sulfonylurea) (16.7 + GLB), and low glucose with KCl (3.3 + KCl). Insulin quantification was performed using

the Insulin Ultra-Sensitive HTFR kit, and the insulin levels were measured with the Thermo Fisher Varioskan Lux Microplate Reader. Statistical significance was determined with p-values of ≤ 0.05 (), ≤ 0.01 (), ≤ 0.001 (), and ≤ 0.0001 (****).

Figure 4: Immunofluorescence analysis of beta-cells derived from iPSCs carrying *HNF1A* p.A251T. A: Immunofluorescence images of islet-like clusters from the 1159 control and the A251T. The upper panel A shows representative clusters stained for INS/NKX6.1, while the lower panel in A shows representative clusters stained for INS/PDX1 (confocal microscopy, x40, oil immersion). Scale bar = 100 µm. Red indicates NKX6.1, green indicates insulin, blue indicates DAPI (nuclear stain), and the merge panel shows INS/NKX6.1 immunofluorescence staining (top) and INS/PDX1 (bottom). B: Histogram representing the percentage of cells within the islet-like clusters expressing *INS* (n = 15). C: Percentage of cells within the islet-like clusters expressing *NKX6.1* (n = 15). D: Percentage of cells within the islet-like clusters co-expressing *NKX6.1* and *INS* (n = 9). E: Percentage of cells within the islet-like clusters expressing *PDX1* (n = 9). Statistical significance was determined with p-values of ≤ 0.05 (), ≤ 0.01 (), ≤ 0.001 (), and ≤ 0.0001 (****).

Figure 5: Immunofluorescence staining analysis of islet-like cluster A251T: α-cells-like cells composition. A: Immunostaining of islet-like cells (stage 6, day 25) showing glucagon ((red) and DNA staining with DAPI (blue); scale bar: 100 µm. B: Histogram

representing the percentage of cells within the islet-like clusters expressing glucagon (n = 9). P-value≤ 0.05 (*) indicates statistical significance.

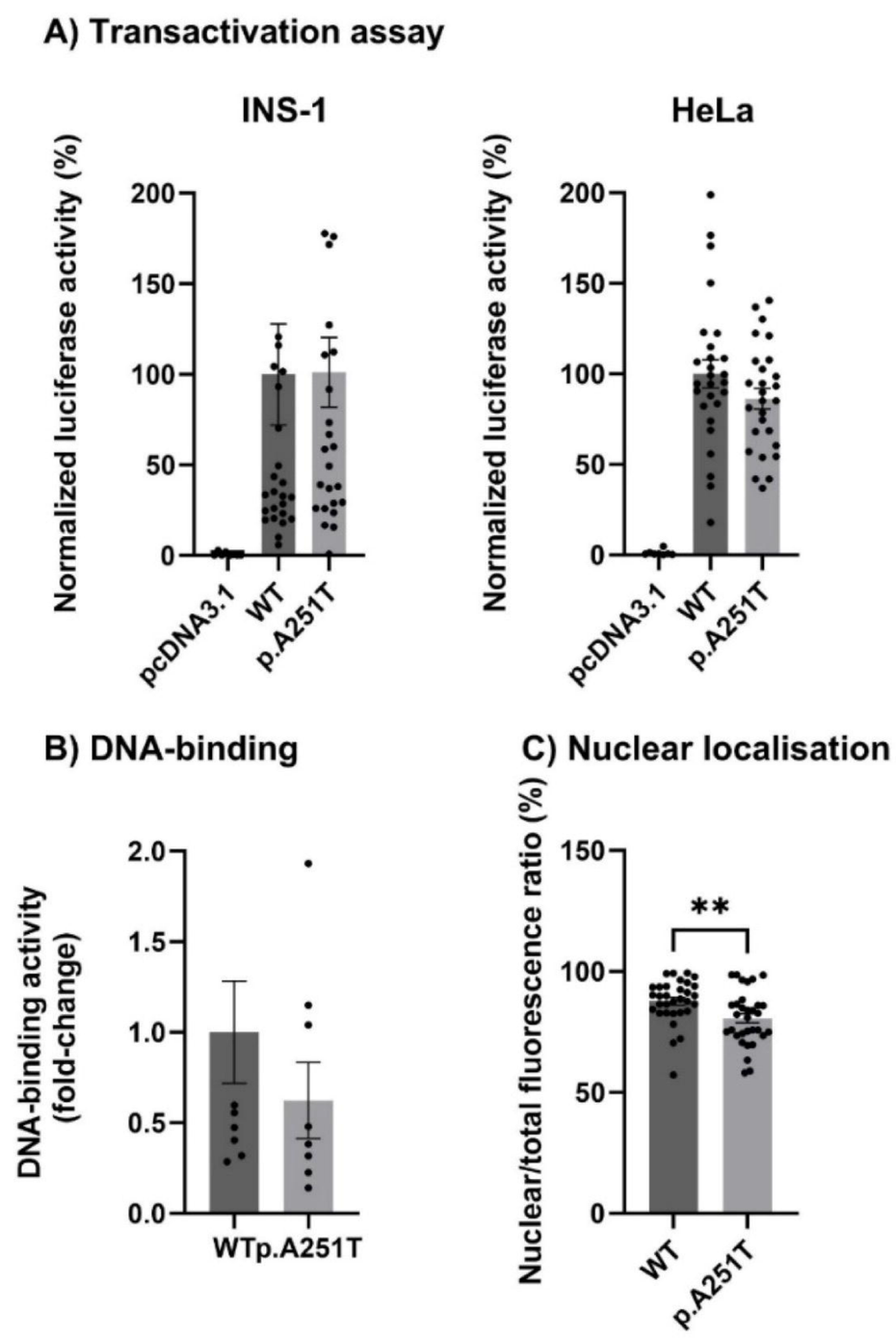
A) Transactivation assay
INS-1
HeLa
Normalized luciferase activity (%)
200
150
100
50
0
pcDNA3.1
WT
p.A251T
B) DNA-binding
DNA-binding activity (fold-change)
2.0
1.5
1.0
0.5
0.0
WTp.A251T
C) Nuclear localisation
Nuclear/total fluorescence ratio (%)
**

Figure 1

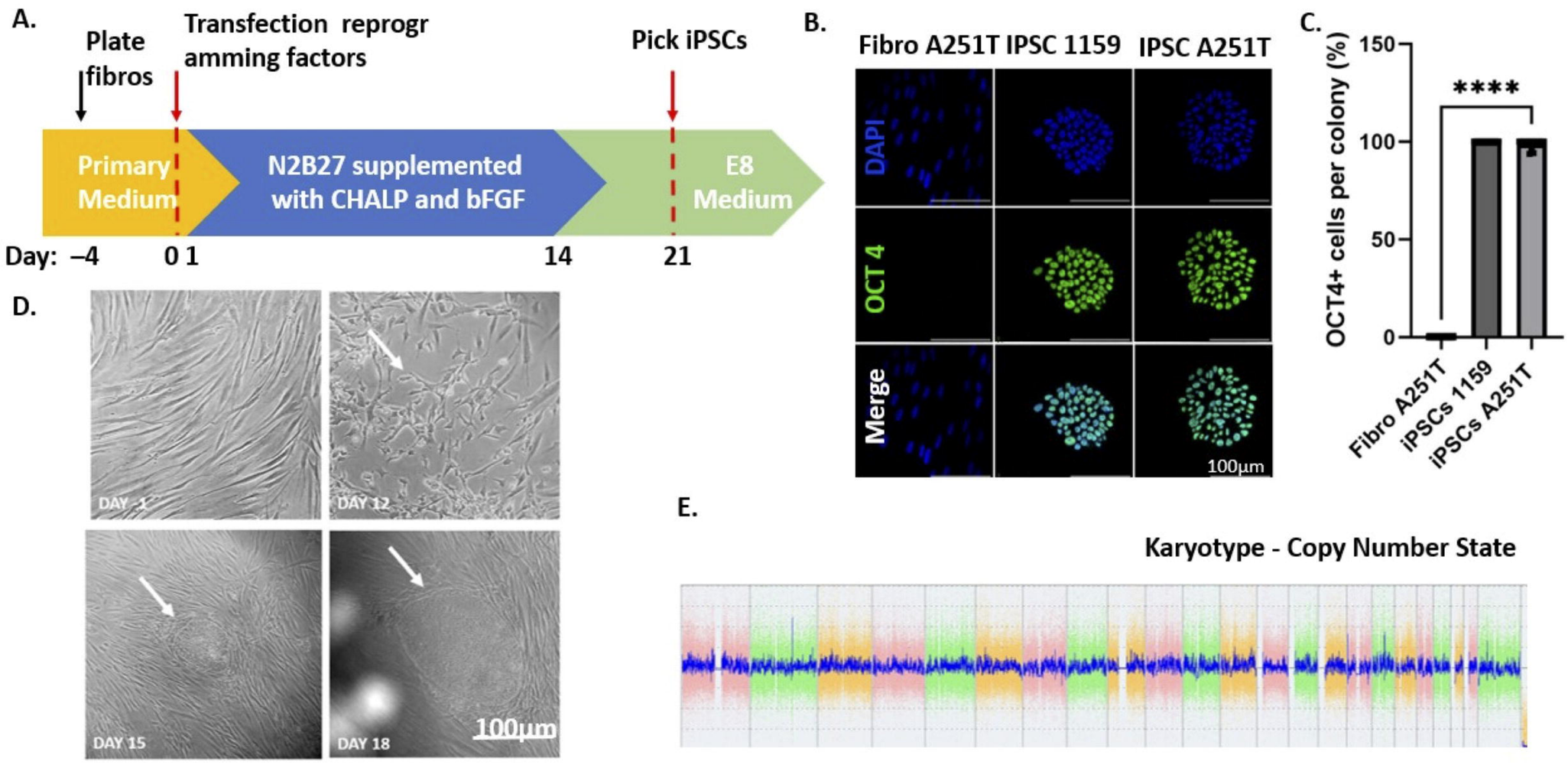
A.
Plate fibros
Transfection reprogr amming factors
Pick iPSCs
Primary Medium
N2B27 supplemented with CHALP and bFGF
E8 Medium
Day: –4
0 1
14
21
B.
Fibro A251T
IPSC 1159
IPSC A251T
DAPI
OCT 4
Merge
100µm
C.
OCT4+ cells per colony (%)
150
100
50
0
****
Fibro A251T
iPSCs 1159
iPSCs A251T
D.
DAY -1
DAY 12
DAY 15
DAY 18
100µm
E.
Karyotype - Copy Number State

Figure 2

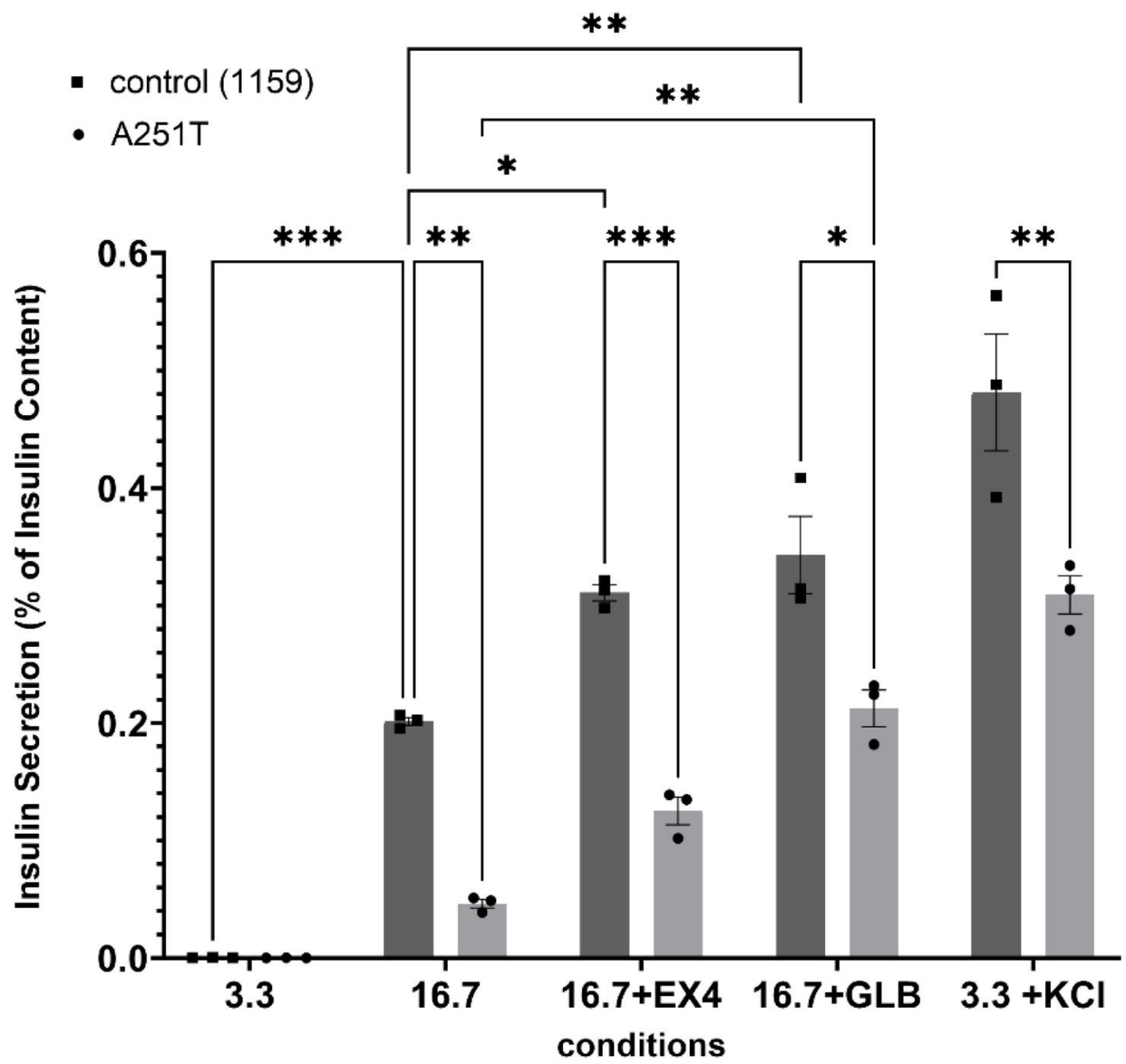
control (1159)
A251T
Insulin Secretion (% of Insulin Content)
0.0
0.2
0.4
0.6
3.3
16.7
16.7+EX4
16.7+GLB
3.3 +KCl
conditions
***
**
***
*
**
*
**
**

Figure 3

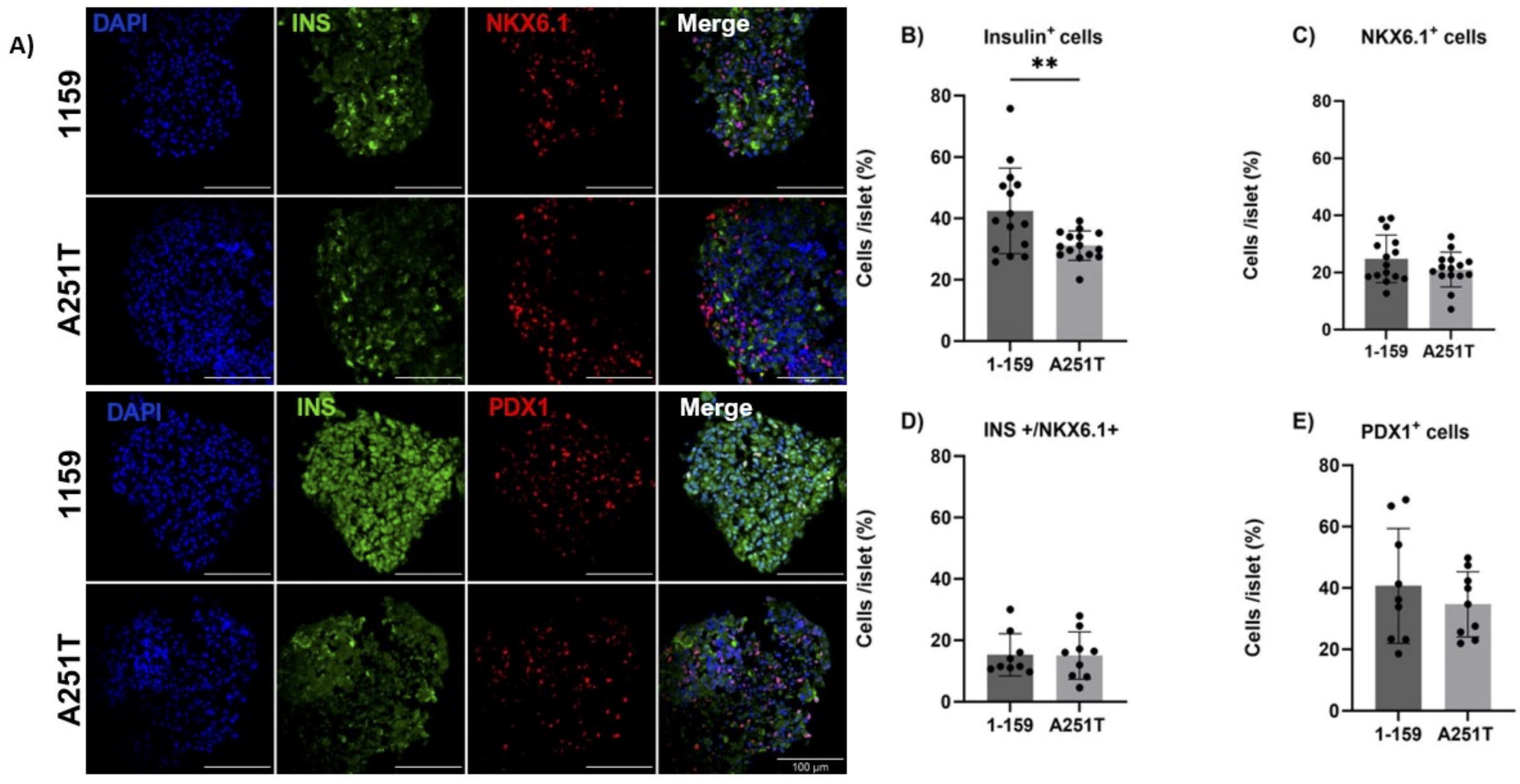
A)
DAPI
INS
NKX6.1
Merge
1159
A251T
DAPI
INS
PDX1
Merge
1159
A251T
100 µm
B)
Insulin⁺ cells
**
Cells /islet (%)
1-159
A251T
C)
NKX6.1⁺ cells
Cells /islet (%)
1-159
A251T
D)
INS +/NKX6.1+
Cells /islet (%)
1-159
A251T
E)
PDX1⁺ cells
Cells /islet (%)
1-159
A251T

Figure 4

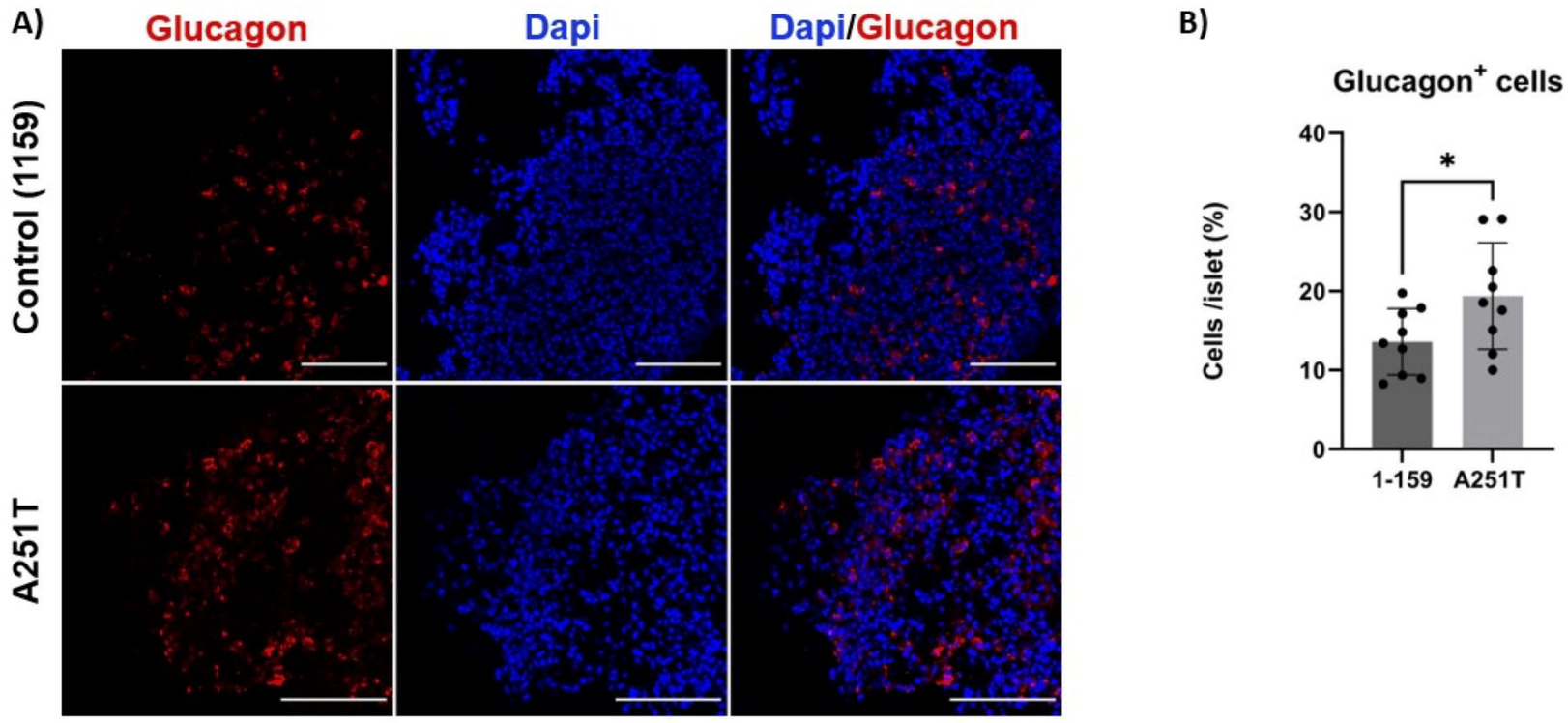
A)
Glucagon
Dapi
Dapi/Glucagon
Control (1159)
A251T
B)
Glucagon+ cells
Cells /islet (%)
40
30
20
10
0
*
1-159
A251T

Figure 5